Clim. Past Discuss., 7, 3859–3893, 2011
www.clim-past-discuss.net/7/3859/2011/
doi:10.5194/cpd-7-3859-2011

Climate of the Past Discussions

Two-signed feedback of cross-isthmus moisture transport on glacial overturning controlled by the Atlantic warm pool

H. J. de Boer[1], D. M. Roche[2,3], H. Renssen[3], and S. C. Dekker[1]

[1]Department of Environmental Sciences, Faculty of Geosciences, Utrecht University, The Netherlands
[2]IPSL/LSCE, CEA-CNRS-UVSQ, Gif-sur-Yvette, France
[3]Faculty of Earth and Life Sciences, VU University Amsterdam, The Netherlands

Received: 27 October 2011 – Accepted: 2 November 2011 – Published: 16 November 2011

Correspondence to: H. J. de Boer (h.j.deboer@uu.nl)

Published by Copernicus Publications on behalf of the European Geosciences Union.

Abstract

This paper studies the control of the Atlantic Warm Pool (AWP) on atmospheric moisture transport across the Central American isthmus as a potential feedback on rapid glacial climate fluctuations. Defined as a region of the Atlantic with surface temperatures above 28.5 °C, the modern AWP expands from the tropical Northwest Atlantic up to the Gulf of Mexico during boreal summer. Due to enhanced deep convection over these warm waters, changes in AWP area cause inverse changes in the strength of the Caribbean low level jet. This low level jet drives atmospheric moisture transport from the Atlantic across the Central American isthmus towards the Pacific. Changes in cross-isthmus moisture transport, potentially related to the AWP, may therefore have affected North Atlantic salinity and the partly density driven Atlantic Meridional Overturning Circulation (AMOC) during the glacial. Based on available proxy evidence we hypothesize that the AWP evolved independent of extratropical North Atlantic temperatures during most of the last glacial, except during periods of AMOC collapse when intense extratropical North Atlantic cooling may have limited eastward AWP expansion. We investigate the implications of this hypothesis for cross-isthmus moisture transport by simulating the coupled ocean-atmosphere response to AMOC collapse and the atmospheric sensitivity to additional variations in AWP area. Our simulations suggest that a decrease in AWP area may increase cross-isthmus moisture transport, whereas extratropical North Atlantic cooling beside a persistent AWP may decrease cross-isthmus moisture transport. Interpretation of these effects throughout an idealized Bond Cycle suggests a positive feedback of reduced cross-isthmus moisture transport in response to Greenland cooling prior to AMOC collapse. During AMOC collapse, when AWP expansion is proposed to have been inhibited, this positive feedback turns negative as enhanced cross-isthmus moisture transport may help AMOC recovery. Supported by reconstructed sea surface salinity changes, we propose that the AWP may have played a key role in the glacial climate by acting as a gatekeeper to regulate moisture transport across the Central American isthmus.

CPD
7, 3859–3893, 2011

1 Introduction

The Atlantic Warm Pool (AWP) is defined as a region of the Atlantic with Sea Surface Temperatures (SSTs) above 28.5 °C (Wang et al., 2006), which is the approximate lower limit for starting deep atmospheric convection (Graham and Barnett, 1987; Zhang, 1993; Fu et al., 1994). At present, the AWP expands from the western tropical North Atlantic into the Caribbean Sea and Gulf of Mexico during boreal summer (Fig. 1a). Paleoclimatic proxy evidence suggests that the AWP persisted to expand into the Gulf of Mexico throughout most of the last glacial (Ziegler et al., 2008). Modern AWP expansion shows considerable variation at interannual and multidecadal timescales linked to El Niño and the Atlantic multidecadal oscillation, respectively, and a secular variation likely linked to global warming (Wang et al., 2008a). These changes in AWP expansion cause same-signed changes in local atmospheric moisture content and inverse changes in the strength of the Caribbean Low Level Jet (CLLJ) due to the enhanced (deep) convection over the warm waters (Wang, 2007; Muñoz et al., 2008; Wang et al., 2008b). The CLLJ is an extension of the North Atlantic subtropical high and forms a local wind maximum in the lower troposphere over the Caribbean Sea due to intensification of the trade winds (Muñoz et al., 2008; Cook and Vizy, 2010). As one of its branches transports atmospheric moisture from the Atlantic across the low-lying Central American isthmus towards the Pacific, the CLLJ may play an important role in the global climate system (Wang et al., 2008a; Richter and Xie, 2010). Changes in cross-isthmus moisture transport may affect North Atlantic salinity, which partly drives northward heat transport by the Atlantic Meridional Overturning Circulation (AMOC) (Broecker et al., 1990; Stocker and Wright, 1991; Rahmstorf, 1996; Lohmann, 2003). Considering that the AWP may evolve both in line with and independent of extratropical North Atlantic temperatures at distinct timescales (Wang et al., 2008a), its control on cross-isthmus moisture transport may provide a mechanism for feedback on the AMOC.

CPD
7, 3859–3893, 2011

Feedbacks between the (sub)tropical atmosphere and the AMOC are relevant from a paleoclimatic perspective because they may have played a key role in abrupt glacial climate change (Broecker, 2003; Goelzer et al., 2006; Chiang, 2009). Abrupt fluctuations in the glacial climate are observed during Dansgaard-Oeschger (D-O) oscillations organized in Bond Cycles (Alley, 1998; Bond et al., 1993; Dansgaard et al., 1993). Heinrich events occur during some of the cold D-O stadials and are recognized by sediment depositions from massive iceberg surges (Heinrich, 1988; Bond et al., 1992). Meltwater from these icebergs may have increased the freshwater forcing on the North Atlantic leading to AMOC slowdown or collapse (Broecker, 1994; Rahmstorf, 1996). Subsequent reduction in northward heat transport resulted in cooling of the extratropical North Atlantic and warming of the tropical and South Atlantic (Stocker, 1998; Ruhlemann et al., 1999; Schmidt et al., 2006; Zarriess et al., 2011). This bipolar SST response likely induced a southward shift of the Intertropical Convergence Zone (ITCZ) and atmospheric drying over the (sub)tropical North Atlantic (Arz et al., 1999; Hemming, 2004; Wang et al., 2004). Accumulation of heat and salt in the tropical Atlantic (Carlson et al., 2008) and the transport of warm and salty waters from the Indian to the South Atlantic Ocean (Weber and Drijfhout, 2007; Chiessi et al., 2008) may have preconditioned the Atlantic for AMOC resumption prior to interstadial warming (Rahmstorf, 2002). Throughout these periods of rapid climate fluctuations, changes in cross-isthmus moisture transport may have acted as a freshwater forcing on the AMOC.

How cross-isthmus moisture transport has affected the glacial AMOC is a topic of current debate (Prange et al., 2010) as evidence exists for both positive and negative feedbacks (Schmidt et al., 2004; Benway et al., 2006; Leduc et al., 2007; Pahnke et al., 2007). This contrast may be reconciled using modern precipitation patterns as analogue, which suggests enhanced transport during warm interstadials and decreased transport during cold Heinrich events (Prange et al., 2010). Alternatively, this inference may be explained by blocking of moisture transport by the Andes when extratropical North Atlantic cooling led to a southward displacement of the ITCZ (Leduc et al., 2007). Although climate models generally reproduce the southward displacement of the ITCZ in response to extratropical North Atlantic cooling (Broccoli et al., 2006), the sign of simulated changes in cross-isthmus moisture transport differs among models (Richter and Xie, 2010). We propose that, beside extratropical North Atlantic temperatures, changes in AWP area may have also affected cross-isthmus moisture prior to and during AMOC collapse.

This paper aims to disentangle how changes in AWP area and extratropical North Atlantic temperatures may have affected cross-isthmus moisture transport as a potential feedback on the glacial AMOC. Hereto we first develop a hypothesis on glacial AWP dynamics based on available paleo-SST reconstructions from the (sub)tropical North Atlantic spanning at least the last 60 kyr. We then simulate the oceanic response to AMOC collapse with a coupled ocean-atmosphere model. Using the simulated surface ocean with hypothesized variations in AWP area as forcing, we perform more detailed atmospheric sensitivity experiments to deconvolve the individual impacts of AWP area and extratropical North Atlantic temperatures on cross-isthmus moisture transport. Simulated changes in cross-isthmus moisture transport are discussed for their potential positive and negative feedbacks in the framework of a conceptual model of the AMOC throughout an idealized Bond Cycle.

2 Proxy evidence for glacial AWP dynamics

To develop a hypothesis on glacial AWP dynamics we use this section to review paleo-SST reconstructions from the (sub)tropical North Atlantic spanning at least the last 60 kyr. The locations and data series of these records are shown in Fig. 1a and b, respectively. SST reconstructions from the warmest part of the modern AWP in the Caribbean Sea indicate a dominant control of summer insolation throughout the last glacial and hint at a slight warming during periods of AMOC collapse (Schmidt et al., 2004). SST reconstructions from the northern edge of the modern AWP in the Gulf of Mexico also indicate a dominant control of summer insolation and show no cooling during periods of AMOC collapse except for Heinrich event 3 (Nurnberg et al., 2008; Ziegler et al., 2008). Reconstructed precipitation increases in Florida may also reflect a warm Caribbean Sea and Gulf of Mexico during periods of AMOC collapse (Donders et al., 2011). Although SST reconstructions from the Iberian margin indicate that the subtropical Northeast Atlantic remained relatively warm throughout most of the glacial, cooling is observed during cold D-O stadials, Heinrich events and the Younger Dryas (Bard et al., 2000; Salgueiro et al., 2010). The strongest cooling (8–14 °C) is recorded during Heinrich events and the Younger Dryas, while less cooling (0–4 °C) is recorded during cold D-O stadials, especially in the southernmost core (MD95-2042). Warming is observed off the coast of West Africa during Heinrich events (Zarriess et al., 2011), reflecting the bi-polar SST response in Atlantic SSTs to AMOC collapse. Based on this evidence we hypothesize that the AWP evolved independent of North Atlantic temperatures during most of the last glacial, except during periods of AMOC collapse when intense North Atlantic cooling hindered eastward AWP expansion beyond the Caribbean Sea and Gulf of Mexico.

3 Methods

3.1 Model framework

To investigate how hypothesized AWP dynamics may control the potential feedbacks between cross-isthmus moisture transport and the glacial AMOC we used two model setups. First, the glacial climate and its response to AMOC collapse resulting from additional freshwater input in the North Atlantic was simulated using the coupled ocean-atmosphere model LOVECLIM version 1.0 (Opsteegh et al., 1998; Goosse and Fichefet, 1999; Goosse et al., 2010). The freshwater forcing in the North Atlantic to evoke AMOC collapse is described in more detail by Roche et al. (2010). LOVECLIM is used here with three components activated: atmosphere (ECBilt), ocean (CLIO) and vegetation (VECODE). In the following, experiments performed with LOVECLIM are named with the prefix “CLIO-” because we mainly focus on its oceanic response. Under glacial boundary conditions with functioning AMOC, the CLIO-LGM simulation presents a small AWP of 1×10^6 km^2 during summer. After AMOC collapse, the CLIO-OFF simulation presents an (insignificant) AWP of 0.2×10^6 km^2 during summer (Fig. 2a).

Second, we performed six sensitivity experiments with the atmospheric General Circulation Model (GCM) PUMA version 2 (Fraedrich et al., 2005a, b) to simulate the effect of AWP area changes on cross-isthmus moisture transport. These simulations were forced using 50-yr transient monthly fields of SSTs and sea-ice cover obtained from CLIO prior to and after AMOC collapse with additional variations in AWP area. An overview of these simulations is presented in Table 1. Seasonal dynamics of AWP area in each simulation are presented in Fig. 2a. We acknowledge that these atmospheric sensitivity experiments were performed in an uncoupled atmospheric GCM, which does not allow to fully resolve feedbacks between cross-isthmus moisture transport and the glacial AMOC. To interpret the simulated changes in cross-isthmus moisture transport as potential feedbacks on the glacial AMOC, the results are discussed in the framework of a conceptual model of the AMOC (Stommel, 1961; Rahmstorf, 1996) throughout an idealized Bond Cycle (Bond et al., 1993; Alley, 1998).

The atmospheric sensitivity simulations used surface ocean output from the CLIO-LGM and CLIO-OFF simulations as a basis for their surface ocean forcing. The LGM^N and OFF^N simulations used CLIO output with no (N) additional AWP area dynamics. For the other atmospheric simulations, variations in AWP area were simulated by replacing the zonal SST gradients in the (sub)tropical North Atlantic (between 5° N and 30° N) in CLIO by modern zonal SST gradients observed during years with small and large AWPs. Following Wang et al. (2008b), a small (large) AWP is defined as being 1/3 smaller (larger) than the average modern AWP in the months July through October. Modern SSTs are derived from the HadISST dataset and the years 1949–2006 (Rayner et al., 2006). Accordingly, the years 1974, 1975, 1976, 1984, 1985 represent small AWPs and the years 1958, 1996, 1997, 1998, 2005, 2006 represent large AWPs. These years were averaged to create one-year composites of monthly SST

CPD
7, 3859–3893, 2011

gradients representative for a small and a large AWP. As the CLIO-LGM simulation produces a warmer subtropical North Atlantic than the CLIO-OFF simulation, replacing their respective zonal SST gradients with the same modern SST gradients results in differently sized AWPs. The atmospheric sensitivity experiments with additional AWP dynamics are therefore named according to the relative size of their AWP. Replacing zonal SST gradients from a small and large AWP for the SST gradients in the CLIO-OFF simulation output results in a small (S) and large (L) AWP in the OFF^S and OFF^L simulations, respectively. The same operation for the CLIO-LGM simulation output results in a large (L) and extra-large (XL) AWP in the LGM^L and LGM^{XL} simulations, respectively. Monthly mean AWP area for each experiment is shown in Fig. 2a. Note that the LGM^L and OFF^L simulations have comparable AWP area and are termed (L) accordingly.

Further, PUMA was used at a T42 resolution with 10 vertical layers, which represents a horizontal resolution of approximately 2.8° latitude by 2.8° longitude. We note that a higher spatial resolution may be required to simulate the detailed flow patterns over the isthmus. However, smoothing of the orography associated with a T42 resolution may partly compensate for potential bias when moisture transport is considered (Xu et al., 2005; Richter and Xie, 2010). All atmospheric simulations were forced with constant Last Glacial Maximum (LGM, 21 kyr BP) boundary conditions for ice-sheet cover and orography (Paul and Schäfer-Neth, 2003), solar insolation and atmospheric CO_2 for which a value of 160 ppmv is used to account for the combined radiative forcing of atmospheric CO_2 and CH_4. Each atmospheric simulation was spun-up by repeating the first simulation year 10 times to minimize the impact of initialization.

3.2 Moisture transport calculations

To evaluate how atmospheric moisture transport simulated by PUMA responds to changes in surface ocean boundary conditions we also performed a modern climate control simulation (CTR) to compare with a modern climate ERA-40 reanalysis (Uppala et al., 2005). The CTR simulation was forced with a composite seasonal cycle

CPD
7, 3859–3893, 2011

of modern monthly SSTs and sea-ice obtained from Rayner et al. (2003). As a measure to evaluate the model with, we calculate low-level zonal moisture transport (Q_Z (g kg^{-1} m s^{-1})) averaged between the surface and the 700 hPa level and over the width of the Atlantic basin as:

$$Q_Z = \overline{q \cdot u} \quad (1)$$

where q is the atmospheric specific humidity (g kg^{-1}) and u (m s^{-1}) is zonal wind speed. Note that easterly flow and transport are indicated by negative values.

Q_Z over the Atlantic basin is dominated by easterly transport between 30° S and 30° N and westerly transport at higher latitudes in the modern climate ERA-40 reanalysis (Fig. 2b). Although PUMA simulates less intense Q_Z over the (sub)tropical North Atlantic in the CTR simulation compared to the ERA-40 reanalysis, the spatial pattern in Q_Z is reproduced. Using glacial boundary conditions of the LGM^N simulation results in stronger than modern easterly Q_Z between the equator and 20° N owing to increased trade winds. Weaker than modern easterly Q_Z is simulated in the Southern Hemisphere between the equator and 15° S. This might be related to atmospheric drying and a decrease in easterly trade winds combined, linked to a southward displacement of the glacial ITCZ relative to the modern CTR simulation. These responses are commonly observed in glacial climate simulations (Kim et al., 2002; Chiang, 2009) and proxy data (Peterson et al., 2000; McGee et al., 2010), which support using PUMA for simulating changes in glacial atmospheric moisture transport.

Our following focus on the (sub)tropical Northwest Atlantic is motivated by the potential feedbacks between cross-isthmus moisture transport and the glacial AMOC. Low level moisture transport (Q (g kg^{-1} m s^{-1})) averaged between the surface and the 700 hPa level is calculated as:

$$Q = \overline{q \cdot \sqrt{u^2 + v^2}} \quad (2)$$

where v (m s^{-1}) is meridional wind speed.

CPD
7, 3859–3893, 2011

Two-signed moisture feedback with the glacial AMOC

H. J. de Boer et al.

Annual average low level cross-isthmus moisture transport dominated by the CLLJ (Q_{CLLJ} (Sv $= 10^6\,\mathrm{m}^3\,\mathrm{s}^{-1}$)) is calculated from Q perpendicular to the line segments 1–4 over the Atlantic-Pacific drainage divide (Fig. 3a) following Xu et al. (2005) and Richter and Xie (2010) as:

$$Q_{\mathrm{CLLJ}} = \int_{P_s}^{P_{700}} \int_{L_1}^{L_4} q \sqrt{u^2 + v^2}\, dL \frac{dP}{g} \tag{3}$$

where P_s and P_{700} are the surface and 700 hPa pressure levels, L_1 and L_4 are the line segments 1 and 4, dL (km) is the distance of over the line segments, dP (note, the unit $\mathrm{Pa} = \mathrm{kg\,m^{-1}\,s^{-2}}$) is the pressure difference and g ($\mathrm{m\,s^{-2}}$) is the gravitation constant.

4 Results

In this section we first analyze the atmospheric response to simulated AMOC collapse. Second, we analyze the atmospheric sensitivity to the individual impacts of North Atlantic cooling and AWP area changes. Finally, we disentangle the effects of both factors on cross-isthmus moisture transport using a regression model.

4.1 Atmospheric response to AMOC collapse

The $\mathrm{LGM}^{\mathrm{N}}$ simulation reveals that the easterly flow over the Caribbean Sea is bounded by the North and South American land masses which channel moisture towards the Central American isthmus (Fig. 3a). Over the isthmus, the modelled flow has the distinct shape of the CLLJ (Muñoz et al., 2008) with annual average maximum easterly wind speeds of $8\,\mathrm{m\,s^{-1}}$ over line segments 3 and 4 at the 900 hPa level (Fig. 3b). Note that negative values indicate easterly flow and transport. Maxima in easterly cross-isthmus moisture transport up to $90\,\mathrm{g\,kg^{-1}\,m\,s^{-1}}$ are confined to the core of the CLLJ where the maximum in flow velocity coincides with high atmospheric moisture content.

The seasonal cycle in cross-isthmus moisture transport exhibits distinct winter and summer maxima which track the seasonality in wind speed (Fig. 3c) and atmospheric moisture content (not shown). During winter (December through March) maximum easterly cross-isthmus moisture transport occurs over the southern part of the isthmus over line segments 2–4. During summer (June through September) maximum easterly cross-isthmus moisture transport is displaced northward to line segments 1 and 2. The winter maximum in cross-isthmus moisture transport is dominated by intensification of the CLLJ, whereas the summer maximum is related to a combined increase in atmospheric humidity over the warm waters of the Gulf of Mexico and an intensification of the summer trade winds.

The anomalous atmospheric response to AMOC collapse is revealed by anomalies between the OFF^N and LGM^N simulations (Fig. 3d–f). Note that, relative to the LGM^N simulation, the OFF^N simulation exhibits cooling in both the extratropical and subtropical North Atlantic leading to a decrease in AWP area (Fig. 2a). This cooling in the OFF^N simulation leads to a drying of the atmosphere over the North Atlantic extending over the tropical South Atlantic to 10° S (Fig. 3d), which suggests a southward displacement of the ITCZ. Besides atmospheric drying, a slight decrease in wind speed is simulated over the northern part of the isthmus (line segments 1–2 in Fig. 3e). Note that as the flow over the isthmus is predominantly directed towards the east, positive anomalies indicate a decrease in easterly flow and moisture transport. A slight increase in cross-isthmus moisture transport and wind speed is simulated over the southern part of the isthmus (line segments 3–4) as indicated by the negative anomalies. These effects combined result in a (small) decrease in cross-isthmus moisture transport of approximately 3 g kg^{-1} m s^{-1} between the OFF^N and LGM^N simulations. The seasonal cycle of anomalous cross-isthmus moisture transport shows an intensification of easterly moisture transport in summer related to an increase in wind speed and a weakening during winter related to atmospheric drying (Fig. 3f). These results suggest that the opposing effects of atmospheric drying and strengthening of the CLLJ may compensate and lead to little net change in annual average cross-isthmus moisture transport.

CPD
7, 3859–3893, 2011

4.2 Atmospheric sensitivity experiments

Anomalous atmospheric responses to extratropical North Atlantic cooling without major changes in AWP area are revealed by anomalies between the OFF^L and LGM^L simulations. These (positive) anomalies show a clear decrease in (easterly) cross-isthmus moisture transport of approximately $15\,g\,kg^{-1}\,m\,s^{-1}$ over line segments 3 and 4 (Fig. 4a, b). A small increase in moisture content over the Caribbean Sea might be related to the slightly larger AWP in the OFF^L simulation compared to the LGM^L simulation. The prominent decrease in cross-isthmus moisture transport is related to a reduction in surface pressure gradient over the Caribbean Sea which weakens the flow over the isthmus (Fig. 4b). The seasonal cycle of cross-isthmus moisture transport shows a year-round decrease (Fig. 4c) due to a weakening of the CLLJ. These results suggest that cooling in the extratropical North Atlantic without major changes in AWP area may considerably reduce cross-isthmus moisture transport.

Anomalous atmospheric responses to a decrease in AWP area are revealed by anomalies between the OFF^S and OFF^L simulations. These (negative) anomalies show a clear increase in (easterly) cross-isthmus moisture transport of approximately $15\,g\,kg^{-1}\,m\,s^{-1}$ over line segments 3 and 4 despite a decrease in atmospheric moisture content in this region (Fig. 4d, e). The increase in cross-isthmus moisture transport is related to steepening of the surface pressure gradient over the subtropical Northeast Atlantic, resulting in an intensification of the CLLJ (Fig. 4e). The increase in easterly cross-isthmus moisture transport occurs year-round, but anomalies extend further northward during boreal summer (Fig. 4f). A minor decrease in easterly cross-isthmus moisture transport is simulated north of the core of the CLLJ over line segments 1 and 2 owing to a decrease in atmospheric moisture content and a reduction in cross-isthmus wind speed. Although anomalies between the LGM^L and LGM^{XL} simulations are not shown, they are comparable to the anomalies between the OFF^S and OFF^L simulations. These results suggest that the increase in simulated cross-isthmus moisture transport in response to a decrease in AWP area is related to strengthening of the CLLJ.

4.3 Simplified GCM response

Our atmospheric sensitivity experiments reveal that extratropical North Atlantic temperatures and AWP area both affect cross-isthmus moisture transport by the CLLJ. To disentangle the individual effects of both factors, we construct a simple linear regression model with summer average AWP area (A_{AWP} (km^2)) and annual average Greenland temperatures (T_G (°C)) as predicting variables for annual average simulated cross-isthmus moisture in the core of the CLLJ (Q_{CLLJ} (Sv)):

$$Q_{CLLJ} = \beta_1 + \beta_2 \cdot T_G + \beta_3 \cdot A_{AWP} \tag{4}$$

Note that Greenland temperatures are used as input to reflect extratropical North Atlantic temperatures in order to facilitate interpretation of these results with available Greenland temperature reconstructions. Furthermore, easterly moisture transport by the CLLJ is now defined positive because no westerly transport occurs on average. With the model input presented in Fig. 5a, the best fit with the GCM response ($r^2 = 0.70$, Fig. 5b) is obtained with regression coefficients: $\beta_1 = 0.41$ Sv, $\beta_2 = 3.3 \times 10^{-3}$ Sv °C^{-1}, $\beta_3 = -8.4 \times 10^{-3}$ Sv $(10^6 \times \text{km}^2)^{-1}$. We stress that this regression model is not used predicatively, but rather as a tool to facilitate interpretation of the response of the atmospheric GCM.

Although the regression model underestimates interannual variability in cross-isthmus moisture transport simulated by the GCM (compare standard deviations in Fig. 5c), its fit to the GCM output suggests that extratropical North Atlantic temperatures and AWP area both exert crucial control on cross-isthmus moisture transport. The individual effect of extratropical North Atlantic temperatures is positive, thus cooling leads to a reduction in simulated cross-isthmus moisture transport. Concurringly, the individual effect of AWP area changes is negative, thus a reduction in AWP area leads to an increase in simulated cross-isthmus moisture transport. The combined effect

CPD
7, 3859–3893, 2011

of extratropical North Atlantic temperatures and AWP area on cross-isthmus moisture transport is visualized in Fig. 5d.

To structure our interpretation of the regression model, we analyze its response in the order of events of an idealized Bond Cycle (Bond et al., 1993; Alley, 1998). This idealized climate cycle consists of multiple D-O oscillations on the backdrop of a long-term cooling trend in Greenland linked to growing of the Laurentide Ice Sheet. The cooling trend ends with a Heinrich event that reduces the ice sheet, leads to AMOC shutdown and, according to our hypothesis, inhibition of AWP expansion due to intense extratropical North Atlantic cooling. After AMOC recovery, Greenland warms and a new cycle may begin. The regression model suggests that if Greenland cooling occurred on the backdrop of a persistent AWP, reduced cross-isthmus moisture transport may accumulate to an anomalous (positive) freshwater forcing of approximately 25 mSv considering a 8 °C cooling, as indicated by the arrow between Roman numerals I and II in Fig. 5d. This reduction in moisture transport may be reversed when AWP expansion is inhibited by approximately 3×10^6 km^2, as indicated by the arrow between II and III in Fig. 5d. If the AMOC resumes and AWP expansion lags Greenland warming, cross-isthmus moisture transport may further increase. Eventually, resumed AWP expansion may neutralize this increase in cross-isthmus moisture transport, as indicated by the arrow between III and I in Fig. 5d.

5 Discussion

In this section we first interpret simulated changes in cross-isthmus moisture transport for their potential feedbacks on the glacial AMOC. We then discuss proxy evidence for changes in cross-isthmus moisture transport during periods of rapid glacial climate change. Finally, we discuss our model framework and make recommendations for future study.

5.1 Two-signed feedback with the glacial AMOC

Our results suggest a two-signed response in cross-isthmus moisture transport to extratropical North Atlantic temperature and AWP area changes. This response may constitute a positive or negative feedback with the AMOC depending on whether it reinforces or counteracts a change, respectively. We propose that a positive feedback may occur if the extratropical North Atlantic cools without affecting the AWP. The subsequent reduction in cross-isthmus moisture transport may (further) weaken the AMOC and amplify North Atlantic cooling due to reduced northward heat transport. A negative feedback may occur after AMOC collapse when intense North Atlantic cooling reaches the subtropics and inhibits AWP expansion. The resulting increase in cross-isthmus moisture transport may aid AMOC resumption to restore northward heat transport. These potential positive and negative feedbacks are schematized in Fig. 6a.

The consequences of these potential feedbacks are discussed in the framework of a conceptual model of the AMOC (Stommel, 1961; Rahmstorf, 1996). This conceptual model suggests that the AMOC may be driven by salt and heat (thermohaline regime), by heat only (thermal regime) or by salt only (saline regime) (Fig. 6b). On the premise that the glacial AMOC was either in the thermohaline or thermal regime (Adkins et al., 2002; Prange et al., 2002), a reduction in freshwater export or increase in freshwater import may lead to AMOC collapse. Estimates of AMOC stability are model dependent, but model intercomparison suggest that the modern AMOC requires a freshwater forcing between 0.1 to 0.5 Sv to reach the Stommel bifurcation point of collapse. Despite that the glacial AMOC might have been closer to this point (Weber and Drijfhout, 2007), the simulated decrease in cross-isthmus moisture transport of approximately 25 mSv in response to extratropical North Atlantic cooling is likely not sufficient to cause AMOC collapse on its own. However, diminishing cross-isthmus moisture transport has the potential to bring the glacial AMOC closer to collapse during the gradual cooling phase of a Bond cycle and, subsequently, make the AMOC more vulnerable to collapse by other sources of freshwater input (Romanova et al., 2004). A “weak cycle” of similar magnitude has been proposed by Ganopolski and Rahmstorf (2001) to explain the apparent periodicity in D-O oscillations. This potential positive feedback of reduced cross-isthmus moisture transport on the glacial AMOC is indicated in Fig. 6b between Roman numerals I and II.

Cooling in the extratropical North Atlantic after AMOC collapse may further reduce cross-isthmus moisture transport as long as the AWP continues to expand. However, once cooling in the North Atlantic is severe enough to reach the subtropical North Atlantic via the Canary Current (Zhao et al., 1995; Bard et al., 2000), our simulations suggest that hindered AWP expansion could intensify the CLLJ and increase cross-isthmus moisture transport. This response is in line with the modern inverse relation between cross-isthmus moisture transport and AWP area (Wang, 2007; Wang et al., 2008b). The initially positive feedback therefore turns negative to aid AMOC resumption if AWP expansion is inhibited, as indicated in Fig. 6b between Roman numerals II and III. Together with, for example, additional saltwater import around the southern tip of Africa (Weber and Drijfhout, 2007; Chiessi et al., 2008) and precipitation anomalies over the tropical Atlantic (Krebs and Timmermann, 2007) these negative feedbacks might explain rapid AMOC recovery from a collapsed state (McManus et al., 2004; Gherardi et al., 2009).

Restored northward heat transport after AMOC resumption allows for rapid North Atlantic warming towards interstadial conditions, as observed in Greenland ice-cores (NGRIP-Members, 2004). Depending on the response time of the coupled ocean-atmosphere system, a new equilibrium in overturning is reached or overshoot of the AMOC may occur (McManus et al., 2004). If expansion of the AWP lags warming in the extratropical North Atlantic, our simulations suggest that further enhanced cross-isthmus moisture transport may contribute to AMOC overshoot during a warm interstadial. However, this increase in cross-isthmus moisture transport is stabilized once the AWP expands, as indicated in Fig. 6b between Roman numerals III and I.

CPD
7, 3859–3893, 2011

5.2 Proxy evidence for altered moisture transport

Records of Sea Surface Salinity (SSS) near the Central American isthmus may be used to reconstruct changes in cross-isthmus moisture transport based on local precipitation and evaporation fluxes (Benway and Mix, 2004). Comparing SSS reconstructions from the Atlantic and Pacific sides of the isthmus reveals higher salinity on the Atlantic side throughout most of the last glacial (Fig. 7a), which suggests that moisture was transported from the warm evaporative waters of the Caribbean towards the cooler (sub)tropical East Pacific (Schmidt et al., 2004; Benway et al., 2006; Leduc et al., 2007). These records also suggest synchronous SSS increases during Heinrich events, which may be related to reduced precipitation and increased evaporation linked to southward displacement of the ITCZ (Leduc et al., 2007). Leduc et al. (2007) further noted that these salinity increases were larger at the Pacific side of the isthmus than at the Atlantic side (Fig. 7b). By assuming that precipitation at the Pacific side of the isthmus consists of water evaporated in the Atlantic basin, Leduc et al. (2007) argued that cross-isthmus moisture transport was reduced during Heinrich events. Although an opposing result has been obtained using a SSS reconstruction from a more southern location (Pahnke et al., 2007), recent interpretation of these contrasting inferences does suggest that cross-isthmus moisture transport was reduced during Heinrich events (Prange et al., 2010).

As Pacific salinity increases are evident during Heinrich events, Pacific salinity decreases shortly after Heinrich events may also suggest an increase in cross-isthmus moisture transport (Fig. 7a). Furthermore, we suggest that part of the variability observed between salinity increases on both sides of the isthmus may be related to the AWP. To test this proposition, we use a SST reconstruction from the Gulf of Mexico as a proxy for AWP expansion at the onset of AMOC collapse (Ziegler et al., 2008) (Fig. 7b). A positive correlation is apparent between this temperature and the reduction in reconstructed cross-isthmus moisture transport during periods of AMOC collapse (calculated as Pacific minus Caribbean salinity increase, Fig. 7c). Although this evidence may be circumstantial, it could support our model inference that a decrease in cross-isthmus moisture transport due to extratropical North Atlantic cooling may be amplified by the AWP.

5.3 Model framework

The aim of this study was to disentangle how AWP area and extratropical North Atlantic temperatures may have affected cross-isthmus moisture transport as a potential feedback on the glacial AMOC. We acknowledge that our model setup does not allow to fully couple changes in cross-isthmus moisture transport to the AMOC. However, by separating atmospheric responses to extratropical North Atlantic cooling from those to AWP area changes, we were able to study the sensitivity in cross-isthmus moisture transport. It could be argued that a higher resolution atmospheric model is required to resolve the detailed flow across the isthmus (Xu et al., 2005; Richter and Xie, 2010). However, the simulated response of the CLLJ to AWP area changes is comparable to modern climate reanalysis data (Wang, 2007) and the accumulated moisture transport matches other estimates (Richter and Xie, 2010). Rather, our results emphasize the importance to constrain glacial AWP dynamics with additional empirical evidence. Future focus should also be on correctly resolving AWP dynamics when simulating periods of abrupt glacial climate change. Eddy-resolving detail might be required to simulate wind-driven driven currents through the Caribbean Sea (Johns et al., 2002) and the Loop Current in the Gulf of Mexico (Chang and Oey, 2011). Moreover, the cold SST bias of coupled ocean-atmosphere models in the (sub)tropical Northwest Atlantic could be problematic to resolve glacial AWP dynamics (Pailler et al., 1999; Breugem et al., 2008; Otto-Bliesner et al., 2009). Due to the critical threshold of 28.5 °C for starting deep atmospheric convection (Fu et al., 1994; Graham and Barnett, 1987; Zhang, 1993), even a small cold SST bias in the (sub)tropical Northeast Atlantic could result in underestimation of changes in the CLLJ. We therefore suggest that a realistic AWP is a crucial requirement for coupled ocean-atmosphere models to resolve feedbacks between cross-isthmus moisture transport and the glacial AMOC.

6 Conclusions

We propose that the AWP may have played a key role in the glacial climate by acting as a gatekeeper to regulate atmospheric moisture transport from the Atlantic across the Central American isthmus towards the Pacific. Central to this role is the inverse relationship between AWP area and the strength of the CLLJ which drives moisture transport across the low-lying isthmus. The resulting changes in the North Atlantic freshwater forcing may have constituted a two-signed feedback with the AMOC prior to and during rapid glacial climate fluctuations.

Acknowledgements. We sincerely thank Gert-Jan Reichart and Maarten B. Eppinga for their insightful comments that greatly improved this manuscript. This research was funded by the High Potential project of Utrecht University.

References

Adkins, J. F., McIntyre, K., and Schrag, D. P.: The salinity, temperature, and δ^{18}O of the Glacial Deep Ocean, Science, 298, 1769–1773, doi:10.1126/science.1076252, 2002.

Alley, R. B.: Palaeoclimatology: Icing the North Atlantic, Nature, 392, 335–337, doi:10.1038/32781, 1998.

Arz, H. W., Pätzold, J., and Wefer, G.: The deglacial history of the western tropical Atlantic as inferred from high resolution stable isotope records off Northeastern Brazil, Earth Planet. Sci. Lett., 167, 105–117, doi:10.1016/S0012-821X(99)00025-4, 1999.

Bard, E., Rostek, F., Turon, J.-L., and Gendreau, S.: Hydrological Impact of Heinrich Events in the Subtropical Northeast Atlantic, Science, 289, 1321–1324, doi:10.1126/science.289.5483.1321, 2000.

Benway, H. and Mix, A. C.: Oxygen isotopes, upper-ocean salinity, and precipitation sources in the Eastern tropical Pacific, Earth Planet. Sci. Lett., 224, 493–507, doi:10.1016/j.epsl.2004.05.014, 2004.

Benway, H., Mix, A. C., Haley, B. A., and Klinkhammer, G. P.: Eastern Pacific warm pool paleosalinity and climate variability: 0–30 kyr, Paleoceanography, 21, 11, doi:10.1029/2005PA001208, 2006.

Bond, G., Heinrich, H., Broecker, W., Labeyrie, L., McManus, J., Andrews, J., Huon, S., Jantschik, R., Clasen, S., Simet, C., Tedesco, K., Klas, M., Bonani, G., and Ivy, S.: Evidence for massive discharges of icebergs into the North Atlantic ocean during the last glacial period, Nature, 360, 245–249, 1992.
Bond, G., Broecker, W., Johnsen, S., McManus, J., Labeyrie, L., Jouzel, J., Bonani, G., and Ivy, S.: Correlations between climate records from North Atlantic sediments and Greenland ice, Nature, 365, 143–147, doi:10.1038/365143a0, 1993.
Breugem, W.-P., Chang, P., Jang, C. J., Mignot, J., and Hazeleger, W.: Barrier layers and tropical Atlantic SST biases in coupled GCMs, Tellus A, 60, 885–897, doi:10.1111/j.1600-0870.2008.00343.x, 2008.
Broccoli, A. J., Dahl, K. A., and Stouffer, R. J.: Response of the ITCZ to Northern Hemisphere cooling, Geophys. Res. Lett., 33, 4, doi:10.1029/2005GL024546, 2006.
Broecker, W. S.: Massive iceberg discharges as triggers for global climate change, Nature, 372, 421–424, doi:10.1038/372421a0, 1994.
Broecker, W. S.: Does the trigger for abrupt climate change reside in the ocean or in the atmosphere?, Science, 300, 1519–1522, doi:10.1126/science.1083797, 2003.
Broecker, W. S., Bond, G., Klas, M., Bonani, G., and Wolfli, W.: A salt oscillator in the glacial Atlantic? 1. The concept, Paleoceanography, 5, 469–477, doi:10.1029/PA005i004p00469, 1990.
Carlson, A. E., Oppo, D. W., Came, R. E., LeGrande, A. N., Keigwin, L. D., and Curry, W. B.: Subtropical Atlantic salinity variability and Atlantic meridional circulation during the last deglaciation, Geology, 36, 991–994, doi:10.1130/G25080A.1, 2008.
Chang, Y.-L. and Oey, L.-Y.: Loop Current Cycle: Coupled Response of the Loop Current with Deep Flows, Journal of Physical Oceanography, 41, 458–471, doi:10.1175/2010JPO4479.1, 2011.
Chiang, J. C. H.: The Tropics in Paleoclimate, Annu. Rev. Earth Planet. Sci., 37, 263–297, doi:10.1146/annurev.earth.031208.100217, 2009.
Chiessi, C. M., Mulitza, S., Paul, A., Patzold, J., Groeneveld, J., and Wefer, G.: South Atlantic interocean exchange as the trigger for the Bolling warm event, Geology, 36, 919–922, doi:10.1130/G24979A.1, 2008.
Cook, K. H. and Vizy, E. K.: Hydrodynamics of the Caribbean low-level jet and its relationship to precipitation, J. Climate, 23, 1477–1494, doi:10.1175/2009JCLI3210.1, 2010.
Dansgaard, W., Johnsen, S. J., Clausen, H. B., Dahl-Jensen, D., Gundestrup, N. S., Ham-

CPD
7, 3859–3893, 2011

Two-signed moisture feedback with the glacial AMOC

H. J. de Boer et al.

mer, C. U., Hvidberg, C. S., Steffensen, J. P., Sveinbjornsdottir, A. E., Jouzel, J., and Bond, G.: Evidence for general instability of past climate from a 250-kyr ice-core record, Nature, 364, 218–220, doi:10.1038/364218a0, 1993.

Donders, T. H., Boer, H. J. de, Finsinger, W., Grimm, E. C., Dekker, S. C., Reichart, G.-J., and Wagner-Cremer, F.: Impact of the Atlantic Warm Pool on precipitation and temperature in Florida during North Atlantic cold spells, Clim. Dynam., 36, 109–118, doi:10.1007/s00382-009-0702-9, 2011.

Fraedrich, K., Jansen, H., Kirk, E., and Lunkeit, F.: The Planet Simulator: Green planet and desert world, Meteorologische Z., 14, 305–314, 2005a.

Fraedrich, Jansen, H., Kirk, E., Luksch, U., and Lunkeit, F.: The Planet Simulator: Towards a user friendly model, Meteorologische Z., 14, 299–304, 2005b.

Fu, R., Del Genio, A. D., and Rossow, W. B.: Influence of ocean surface conditions on atmospheric vertical thermodynamic structure and deep convection, J. Climate, 7(7), 1092–1108, 1994.

Ganopolski, A. and Rahmstorf, S.: Rapid changes of glacial climate simulated in a coupled climate model, Nature, 409, 153–158, doi:10.1038/35051500, 2001.

Gesch, D. B., Verdin, K. L., and Greenlee, S. K.: New land surface digital elevation model covers the Earth, Eos Trans. AGU, 80, 69, doi:10.1029/99EO00050, 1999.

Gherardi, J.-M., Labeyrie, L., Nave, S., Francois, R., McManus, J. F., and Cortijo, E.: Glacial-interglacial circulation changes inferred from 231Pa/230Th sedimentary record in the North Atlantic region, Paleoceanography, 24, 14 pp., doi:10.1029/2008PA001696, 2009.

Goelzer, H., Mignot, J., Levermann, A., and Rahmstorf, S.: Tropical versus high latitude freshwater influence on the Atlantic circulation, Clim. Dynam., 27, 715–725, doi:10.1007/s00382-006-0161-5, 2006.

Goosse, H. and Fichefet, T.: Importance of ice-ocean interactions for the global ocean circulation: a model study, J. Geophys. Res., 104, 23337–23355, doi:10.1029/1999JC900215, 1999.

Goosse, H., Brovkin, V., Fichefet, T., Haarsma, R., Huybrechts, P., Jongma, J., Mouchet, A., Selten, F., Barriat, P.-Y., Campin, J.-M., Deleersnijder, E., Driesschaert, E., Goelzer, H., Janssens, I., Loutre, M.-F., Morales Maqueda, M. A., Opsteegh, T., Mathieu, P.-P., Munhoven, G., Pettersson, E. J., Renssen, H., Roche, D. M., Schaeffer, M., Tartinville, B., Timmermann, A., and Weber, S. L.: Description of the Earth system model of intermediate complexity LOVECLIM version 1.2, Geosci. Model Dev., 3, 603–633, doi:10.5194/gmd-3-603-2010,

2010.
Graham, N. E. and Barnett, T. P.: Sea surface temperature, surface wind divergence, and convection over tropical oceans, Science, 238, 657–659, doi:10.1126/science.238.4827.657, 1987.
Grimm, E. C., Watts, W. A., Jacobson Jr., G. L., Hansen, B. C. S., Almquist, H. R., and Dieffenbacher-Krall, A. C.: Evidence for warm wet Heinrich events in Florida, Quaternary Sci. Rev., 25, 2197–2211, doi:10.1016/j.quascirev.2006.04.008, 2006.
Heinrich, H.: Origin and consequences of cyclic ice rafting in the Northeast Atlantic Ocean during the past 130 000 yr, Quaternary Res., 29, 142–152, doi:10.1016/0033-5894(88)90057-9, 1988.
Hemming, S. R.: Heinrich events: Massive late Pleistocene detritus layers of the North Atlantic and their global climate imprint, Rev. Geophys., 42, 43 pp., doi:10.1029/2003RG000128, 2004.
Johns, W. E., Townsend, T. L., Fratantoni, D. M., and Wilson, W. D.: On the Atlantic inflow to the Caribbean Sea, Deep-Sea Res. Pt. 1, 49, 211–243, doi:10.1016/S0967-0637(01)00041-3, 2002.
Kim, S. J., Flato, M. and Boer, G. J.: A coupled climate model simulation of the Last Glacial Maximum, Part 2: approach to equilibrium, Clim. Dynam., 20, 635–661, 2002.
Krebs, U. and Timmermann, A.: Tropical air–sea interactions accelerate the recovery of the atlantic meridional overturning circulation after a major shutdown, J. Climate, 20, 4940–4956, doi:10.1175/JCLI4296.1, 2007.
Leduc, G., Vidal, L., Tachikawa, K., Rostek, F., Sonzogni, C., Beaufort, L., and Bard, E.: Moisture transport across Central America as a positive feedback on abrupt climatic changes, Nature, 445, 908–911, doi:10.1038/nature05578, 2007.
Lohmann, G.: Atmospheric and oceanic freshwater transport during weak Atlantic overturning circulation, Tellus A, 55, 438–449, doi:10.1034/j.1600-0870.2003.00028.x, 2003.
McGee, D., Broecker, W. S., and Winckler, G.: Gustiness: The driver of glacial dustiness?, Quaternary Sci. Rev., 29, 2340–2350, doi:10.1016/j.quascirev.2010.06.009, 2010.
McManus, J. F., Francois, R., Gherardi, J.-M., Keigwin, L. D., and Brown-Leger, S.: Collapse and rapid resumption of Atlantic meridional circulation linked to deglacial climate changes, Nature, 428, 834–837, doi:10.1038/nature02494, 2004.
Muñoz, E., Busalacchi, A. J., Nigam, S., and Ruiz-Barradas, A.: Winter and summer structure of the Caribbean low-level jet, J. Climate, 21, 1260–1276, doi:10.1175/2007JCLI1855.1, 2008.

CPD
7, 3859–3893, 2011

Two-signed moisture feedback with the glacial AMOC

H. J. de Boer et al.

NGRIP-Members: High-resolution record of Northern Hemisphere climate extending into the last interglacial period, Nature, 431, 147–151, doi:10.1038/nature02805, 2004.
Nurnberg, D., Ziegler, M., Karas, C., Tiedemann, R., and Schmidt, M.: Interacting loop current variability and Mississippi River discharge over the past 400 kyr, Earth Planet. Sci. Lett., 272, 278–289, doi:10.1016/j.epsl.2008.04.051, 2008.
Opsteegh, J. D., Haarsma, R. J., Selten, F. M., and Kattenberg, A.: ECBILT: a dynamic alternative to mixed boundary conditions in ocean models, Tellus A, 50, 348–367, doi:10.1034/j.1600-0870.1998.t01-1-00007.x, 1998.
Otto-Bliesner, B. L., Schneider, R., Brady, E. C., Kucera, M., Abe-Ouchi, A., Bard, E., Braconnot, P., Crucifix, M., Hewitt, C. D., Kageyama, M., Marti, O., Paul, A., Rosell-Melé, A., Waelbroeck, C., Weber, S. L., Weinelt, M., and Yu, Y.: A comparison of PMIP2 model simulations and the MARGO proxy reconstruction for tropical sea surface temperatures at last glacial maximum, Clim. Dynam., 32, 799–815, doi:10.1007/s00382-008-0509-0, 2009.
Pahnke, K., Sachs, J. P., Keigwin, L., Timmermann, A., and Xie, S.-P.: Eastern tropical Pacific hydrologic changes during the past 27 ,000 yr from D/H ratios in alkenones, Paleoceanography, 22, 15, doi:10.1029/2007PA001468, 2007.
Pailler, K., Bourlès, B., and Gouriou, Y.: The barrier layer in the western tropical Atlantic Ocean, Geophys. Res. Lett., 26, 2069–2072, doi:10.1029/1999GL900492, 1999.
Paul, A. and Schäfer-Neth, C.: Modeling the water masses of the Atlantic Ocean at the Last Glacial Maximum, Paleoceanography, 18, 26, doi:10.1029/2002PA000783, 2003.
Peterson, L. C., Haug, G. H., Hughen, K. A., and Rohl, U.: Rapid changes in the hydrologic cycle of the tropical Atlantic during the last glacial, Science, 290, 1947–1951, doi:10.1126/science.290.5498.1947, 2000.
Prange, M., Romanova, V., and Lohmann, G.: The glacial thermohaline circulation: stable or unstable?, Geophys. Res. Lett., 29, 4, doi:10.1029/2002GL015337, 2002.
Prange, M., Steph, S., Schulz, M., and Keigwin, L. D.: Inferring moisture transport across Central America: can modern analogs of climate variability help reconcile paleosalinity records?, Quaternary Sci. Rev., 29, 1317–1321, doi:10.1016/j.quascirev.2010.02.029, 2010.
Rahmstorf, S.: On the freshwater forcing and transport of the Atlantic thermohaline circulation, Clim. Dynam., 12, 799–811, doi:10.1007/s003820050144, 1996.
Rahmstorf, S.: Ocean circulation and climate during the past 120 000 years, Nature, 419, 207–214, doi:10.1038/nature01090, 2002.
Rashid, H.: Evidence for an additional Heinrich event between H5 and H6 in the Labrador Sea,

Paleoceanography, 18, 1077–1092, doi:10.1029/2003PA000913, 2003.
Rayner, N. A.: Global analyses of sea surface temperature, sea ice, and night marine air temperature since the late nineteenth century, J. Geophys. Res., 108, 4407–4436, doi:10.1029/2002JD002670, 2003.
Rayner, N. A., Brohan, P., Parker, D. E., Folland, C. K., Kennedy, J. J., Vanicek, M., Ansell, T. J., and Tett, S. F. B.: Improved analyses of changes and uncertainties in sea surface temperature measured in situ since the mid-nineteenth century: the HadSST2 dataset, J. Climate, 19, 446–469, doi:10.1175/JCLI3637.1, 2006.
Richter, I. and Xie, S.-P.: Moisture transport from the Atlantic to the Pacific basin and its response to North Atlantic cooling and global warming, Clim. Dynam., 35, 551–566, doi:10.1007/s00382-009-0708-3, 2010.
Roche, D. M., Wiersma, A. P., and Renssen, H.: A systematic study of the impact of freshwater pulses with respect to different geographical locations, Clim. Dynam., 34, 997–1013, doi:10.1007/s00382-009-0578-8, 2010.
Romanova, V., Prange, M., and Lohmann, G.: Stability of the glacial thermohaline circulation and its dependence on the background hydrological cycle, Clim. Dynam., 22, 527–538, doi:10.1007/s00382-004-0395-z, 2004.
Ruhlemann, C., Mulitza, S., Muller, P. J., Wefer, G., and Zahn, R.: Warming of the tropical Atlantic Ocean and slowdown of thermohaline circulation during the last deglaciation, Nature, 402, 511–514, doi:10.1038/990069, 1999.
Salgueiro, E., Voelker, A. H. L., de Abreu, L., Abrantes, F., Meggers, H., and Wefer, G.: Temperature and productivity changes off the western Iberian margin during the last 150 ky, Quaternary Sci. Rev., 29, 680–695, doi:10.1016/j.quascirev.2009.11.013, 2010.
Schmidt, M. W., Spero, H. J., and Lea, D. W.: Links between salinity variation in the Caribbean and North Atlantic thermohaline circulation, Nature, 428, 160–163, doi:10.1038/nature02346, 2004.
Schmidt, M. W., Vautravers, M. J., and Spero, H. J.: Western Caribbean sea surface temperatures during the late Quaternary, Geochem. Geophys. Geosyst., 7, 17, doi:10.1029/2005GC000957, 2006.
Stocker, T. F.: Climate change: the Seesaw effect, Science, 282, 61–62, doi:10.1126/science.282.5386.61, 1998.
Stocker, T. F. and Wright, D. G.: Rapid transitions of the ocean's deep circulation induced by changes in surface water fluxes, Nature, 351, 729–732, doi:10.1038/351729a0, 1991.

Stommel, H.: Thermohaline convection with two stable regimes of flow, Tellus, 13, 224–230, doi:10.1111/j.2153-3490.1961.tb00079.x, 1961.
Stoner, J. S., Channell, J. E. T., Hillaire-Marcel, C., and Kissel, C.: Geomagnetic paleointensity and environmental record from Labrador Sea core MD95–2024: global marine sediment and ice core chronostratigraphy for the last 110 kyr, Earth Planet. Sci. Lett., 183, 161–177, doi:10.1016/S0012-821X(00)00272-7, 2000.
Uppala, S. M., Kållberg, P. W., Simmons, A. J., Andrae, U., Bechtold, V. D. C., Fiorino, M., Gibson, J. K., Haseler, J., Hernandez, A., Kelly, G. A., Li, X., Onogi, K., Saarinen, S., Sokka, N., Allan, R. P., Andersson, E., Arpe, K., Balmaseda, M. A., Beljaars, A. C. M., Berg, L., Van De, Bidlot, J., Bormann, N., Caires, S., Chevallier, F., Dethof, A., Dragosavac, M., Fisher, M., Fuentes, M., Hagemann, S., Hólm, E., Hoskins, B. J., Isaksen, L., Janssen, P. A. E. M., Jenne, R., McNally, A. P., Mahfouf, J.-F., Morcrette, J.-J., Rayner, N. A., Saunders, R. W., Simon, P., Sterl, A., Trenberth, K. E., Untch, A., Vasiljevic, D., Viterbo, P., and Woollen, J.: The ERA-40 re-analysis, Q. J. Roy. Meteorol. Soc., 131, 2961–3012, doi:10.1256/qj.04.176, 2005.
Wang, C.: Variability of the Caribbean Low-Level Jet and its relations to climate, Clim. Dynam., 29, 411–422, doi:10.1007/s00382-007-0243-z, 2007.
Wang, C., Enfield, D. B., Lee, S.-K., and Landsea, C. W.: Influences of the Atlantic warm pool on Western Hemisphere summer rainfall and atlantic hurricanes, J. Climate, 19, 3011–3028, doi:10.1175/JCLI3770.1, 2006.
Wang, C., Lee, S.-K., and Enfield, D. B.: Atlantic warm pool acting as a link between atlantic multidecadal oscillation and atlantic tropical cyclone activity, Geochem. Geophys. Geosyst., 9, 16, doi:10.1029/2007GC001809, 2008a.
Wang, C., Lee, S.-K., and Enfield, D. B.: Climate response to anomalously large and small atlantic warm pools during the summer, J. Climate, 21, 2437–2450, doi:10.1175/2007JCLI2029.1, 2008b.
Wang, X., Auler, A. S., Edwards, R. L., Cheng, H., Cristalli, P. S., Smart, P. L., Richards, D. A., and Shen, C.-C.: Wet periods in Northeastern Brazil over the past 210 kyr linked to distant climate anomalies, Nature, 432, 740–743, doi:10.1038/nature03067, 2004.
Weber, S. L. and Drijfhout, S. S.: Stability of the atlantic meridional overturning circulation in the last glacial maximum climate, Geophys. Res. Lett., 34, 5, doi:10.1029/2007GL031437, 2007.
Xu, H., Xie, S.-P., Wang, Y., and Small, R. J.: Effects of central american mountains

CPD
7, 3859–3893, 2011

on the eastern pacific winter ITCZ and moisture transport*, J. Climate, 18, 3856–3873, doi:10.1175/JCLI3497.1, 2005.
Zarriess, M., Johnstone, H., Prange, M., Steph, S., Groeneveld, J., Mulitza, S., and Mackensen, A.: Bipolar seesaw in the Northeastern tropical Atlantic during Heinrich stadials, Geophys. Res. Lett., 38, 6, doi:10.1029/2010GL046070, 2011.
Zhang, C.: Large-scale variability of atmospheric deep convection in relation to sea surface temperature in the tropics, J. Climate, 6, 1898–1913, 1993.
Zhao, M., Beveridge, N. A. S., Shackleton, N. J., Sarnthein, M., and Eglinton, G.: Molecular stratigraphy of cores off northwest Africa: Sea surface temperature history over the last 80 Ka, Paleoceanography, 10, 661–675, doi:10.1029/94PA03354, 1995.
Ziegler, M., Nurnberg, D., Karas, C., Tiedemann, R., and Lourens, L. J.: Persistent summer expansion of the Atlantic Warm Pool during glacial abrupt cold events, Nat. Geosci., 1, 601–605, doi:10.1038/ngeo277, 2008.

CPD
7, 3859–3893, 2011

Two-signed moisture feedback with the glacial AMOC

H. J. de Boer et al.

Table 1. Overview of six atmospheric GCM sensitivity simulations, their prescribed AMOC state and additional AWP dynamics used as forcing. The prefix "CLIO-" refers to simulations performed with LOVECLIM.

Simulation	Sea surface forcing
LGM^{N}	CLIO-LGM glacial steady-state AMOC, no additional AWP
LGM^{L}	As LGM^{N}, with additional seasonal dynamics of a small AWP
LGM^{XL}	As LGM^{N}, with additional seasonal dynamics of a large AWP
OFF^{N}	CLIO-OFF glacial collapsed AMOC, no additional AWP
OFF^{S}	As OFF^{N}, with additional seasonal dynamics of a small AWP
OFF^{L}	As OFF^{N}, with additional seasonal dynamics of a large AWP

CPD
7, 3859–3893, 2011

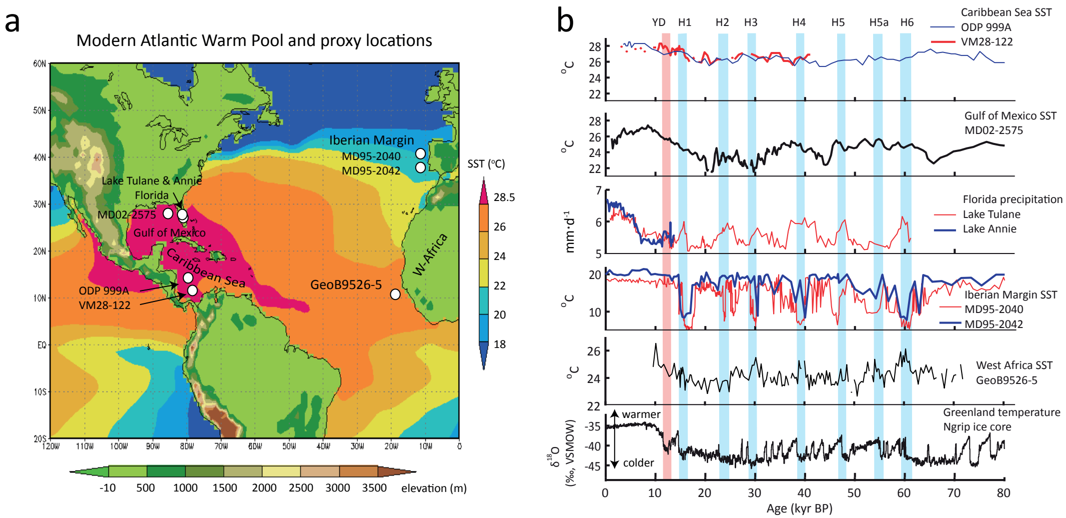

Fig. 1. (a) Modern summer (July through September) SSTs in the (sub)tropical North Atlantic region. SSTs warmer than 28.5 °C are shaded pink to indicate the modern extent of the AWP (Rayner, 2003; Rayner et al., 2006). Plotted surface elevation is based on the GTOPO30 dataset (Gesch et al., 1999). Circles indicate core locations of data series presented in panel **(b)**. **(b)** Paleoclimate proxy reconstructions used to develop a hypothesis on glacial AWP dynamics. Shown from top to bottom are: SSTs in the Caribbean Sea (Schmidt et al., 2004), SSTs in the Gulf of Mexico (Nurnberg et al., 2008; Ziegler et al., 2008), precipitation in Florida reconstructed from Lake Tulane and lake Annie (Grimm et al., 2006; Donders et al., 2011), SSTs from the Iberian margin (Salgueiro et al., 2010) and SSTs off the coast of West Africa (Zarriess et al., 2011) and, Greenland δ^{18}O values representative for Greenland temperatures (NGRIP-Members, 2004). Although the exact timing of Heinrich events varies depending on the records used (Rashid, 2003), coloured bars indicate maximum calendar age ranges of North Atlantic iceberg-rafted debris following Stoner et al. (2000). Blue bars indicate Heinrich events (H1–H6), pink bar indicates the Younger Dryas (YD).

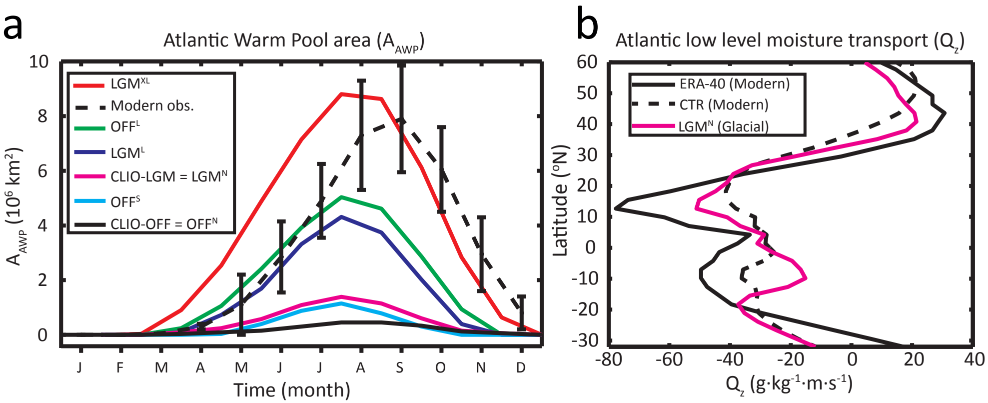

Fig. 2. (a) Seasonal evolution of AWP area in all six atmospheric GCM sensitivity simulations (see Table 1) and modern observations (Rayner et al., 2003, 2006). Error bars denote one standard deviation around the modern monthly mean AWP area. **(b)** Zonal low-level (surface to 700 hPa level) moisture transport (Q_Z (g kg^{-1} m s^{-1})) averaged over the width of the Atlantic basin for the modern ERA-40 reanalysis (Uppala et al., 2005), a modern day control (CTR) simulation and a glacial (LGM^N) simulation.

CPD
7, 3859–3893, 2011

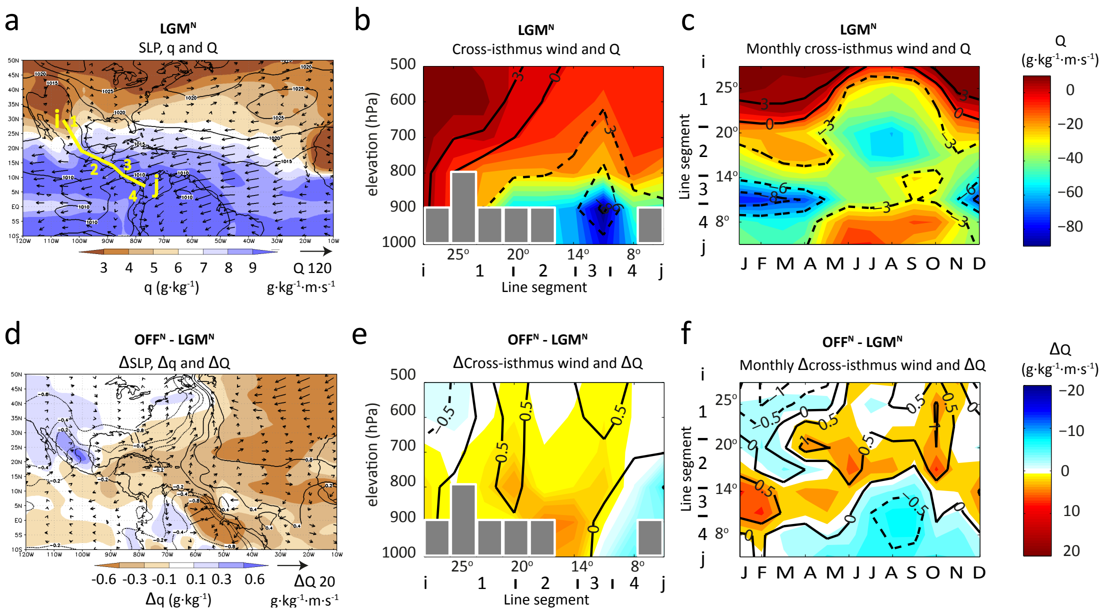

Fig. 3. (a) Annual averages of the LGM^N simulation for sea-level pressure (SLP (hPa)) indicated by contours, atmospheric low-level (surface to 700 hPa level) specific humidity (q (g kg^{-1})) indicated by shading, and low level atmospheric moisture transport (Q (kg kg^{-1} m s^{-1})) indicated by arrows. Line segments 1–4 are used to calculate cross-isthmus moisture transport between points i (30° N, 105° W) and j (7° N, 78° W) in **(b, c)**. **(b)** Annual averages for low level cross-isthmus wind speed ((m s^{-1}) indicated by contours) and cross-isthmus moisture transport (indicated by shading) over the line segments 1–4. Gray bars indicate model orography over the isthmus at each latitude. **(c)** Seasonal cycle in vertically averaged low-level cross-isthmus moisture transport and wind speed. Panels **(d–f)** are as in **(a–c)** but now express anomalies between the OFF^N and LGM^N simulations. Note that westward flow and transport is denoted by negative values. Positive anomalies may therefore reveal a decrease in cross-isthmus flow and transport.

CPD
7, 3859–3893, 2011

Two-signed moisture feedback with the glacial AMOC

H. J. de Boer et al.

Title Page
Abstract | Introduction
Conclusions | References
Tables | Figures
◀| |▶
◀ ▶
Back | Close
Full Screen / Esc
Printer-friendly Version
Interactive Discussion

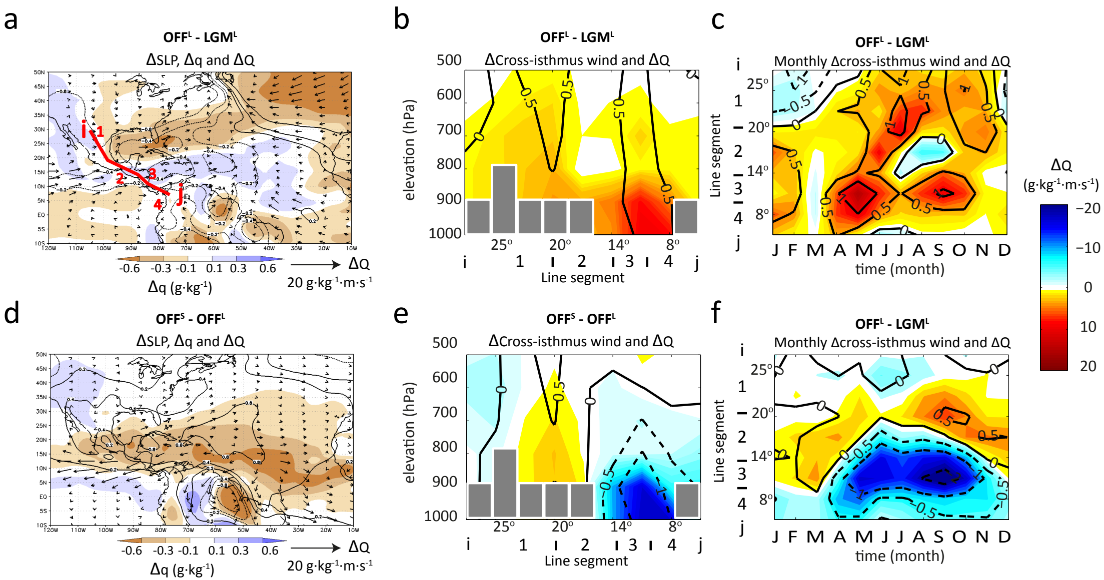

Fig. 4. **(a)** Annual average anomalies between the OFF^L and LGM^L simulations for sea-level pressure (SLP (hPa)) indicated by contours, atmospheric specific humidity (q (g kg^{-1})) indicated by shading, and atmospheric moisture transport (Q (kg kg^{-1} m s^{-1})) indicated by arrows. Line segments 1–4 are used to calculate cross-isthmus moisture transport between points i (30° N, 105° W) and j (7° N, 78° W) in **(b–c)**. **(b)** Annual averages for low level cross-isthmus wind speed ((m s^{-1}) indicated by contours) and cross-isthmus moisture transport (indicated by shading) over line segments 1–4. The gray bars indicate model orography of the isthmus at each latitude. **(c)** Seasonal cycle in vertically averaged low-level cross-isthmus moisture transport and wind speed. Panels **(d–f)** are as in **(a–c)** but now express anomalies between the OFF^S and OFF^L simulations. Note that eastward flow and transport is denoted by positive values. Negative anomalies may therefore reveal an increase in cross-isthmus flow and transport.

CPD
7, 3859–3893, 2011

Two-signed moisture feedback with the glacial AMOC

H. J. de Boer et al.

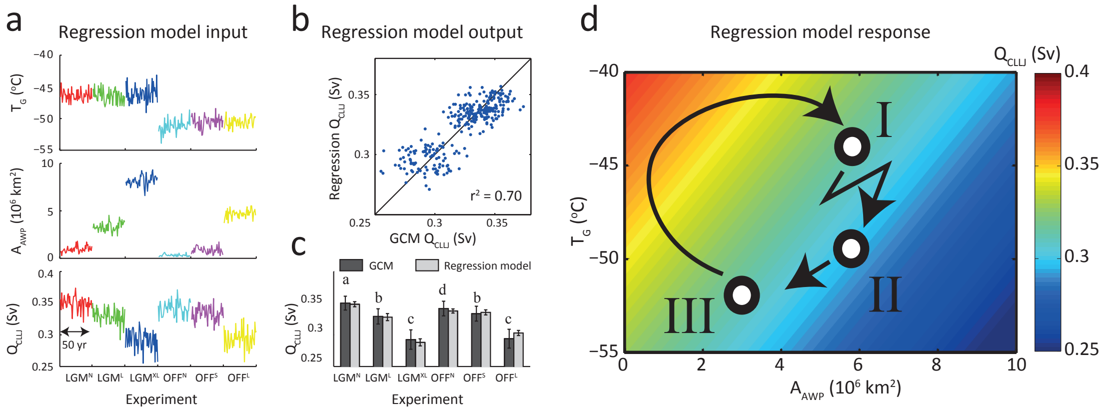

Fig. 5. **(a)** Regression model input is based on annual average Greenland 2 m temperature (T_G (°C)) and summer (JAS) AWP area (A_{AWP} (km^2)) used to predict cross-isthmus moisture transport by the CLLJ (Q_{CLLJ} (Sv)) as simulated by the GCM in all experiments combined (n = 300). **(b)** Best fit of the regressed Q_{CLLJ} to the GCM Q_{CLLJ} ($r^2 = 0.70$). **(c)** Significant differences (using a Student's t-test, $n = 50$) between GCM experiments are indicated. Error bars indicate standard deviations within experiments. **(d)** Regression model response of Q_{CLLJ} as a function of A_{AWP} and T_G. Roman numerals with bullet points indicate the proposed order of events during an idealized Bond cycle (Bond et al., 1992, 1993; Alley, 1998) to aid interpretation of the results. (I → II) Gradual Greenland cooling phase related to the build up of the Laurentide Ice Sheet. (II → III) AMOC collapse during a Heinrich event leading to further Greenland cooling and, as hypothesized, inhibition of AWP expansion. (III → I) AMOC resumption leading to Greenland warming and, eventually, resumed AWP expansion.

CPD
7, 3859–3893, 2011

Two-signed moisture feedback with the glacial AMOC

H. J. de Boer et al.

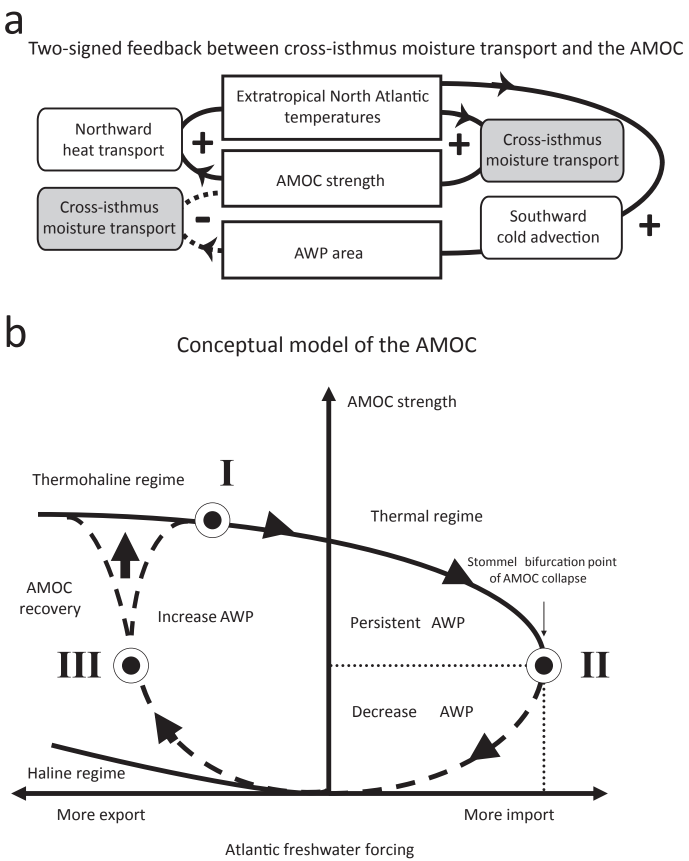

CPD
7, 3859–3893, 2011

Two-signed moisture feedback with the glacial AMOC

H. J. de Boer et al.

Fig. 6. **(a)** Schematic representation of the proposed two-signed feedback between cross-isthmus moisture transport and the glacial AMOC. The (+) and (−) signs denote positive and negative effects, respectively. A positive feedback results from combined effects with an overall positive sign, which reinforces change. A negative feedbacks results from combined effects with an overall negative sign, which counteracts change. According to our simulations, cross-isthmus moisture transport is reduced due to extratropical North Atlantic cooling (+ effect). This may decrease AMOC strength and reduce northward heat transport and, hence, result in further extratropical North Atlantic cooling (+ effect). The overall sign of this feedback (++) is positive. If the AMOC has collapsed and southward advection of cold North Atlantic surface waters may inhibit AWP expansion (+ effect), cross-isthmus moisture transport is enhanced (− effect) to aid AMOC recovery and restore northward heat transport (+ effect). The overall sign of this feedback (+ − +) is negative. **(b)** The potential positive and negative feedbacks are interpreted in the context of a conceptual model of the AMOC (Stommel, 1961; Rahmstorf, 1996). Arrows denote the direction of change induced by the proposed feedbacks. Reduced cross-isthmus moisture transport (less export) due to extratropical North Atlantic cooling may bring a stable thermohaline or thermal flow regime towards the Stommel bifurcation point of AMOC collapse (I → II). Additional freshwater forcing may cause the AMOC to shut down into the unstable regime (dashed lines). The subsequent extratropical North Atlantic cooling may spread southwards and hinder AWP expansion. The freshwater forcing from an increase in cross-isthmus moisture transport (more export) may aid AMOC resumption and act as a negative feedback (II → III). Once the AMOC resumes and the AWP expands, the negative feedback of enhanced cross-isthmus moisture transport is neutralized (III → I). Overshoot of the AMOC may be enhanced if AWP expansion lags extratropical North Atlantic warming.

CPD
7, 3859–3893, 2011

Two-signed moisture feedback with the glacial AMOC

H. J. de Boer et al.

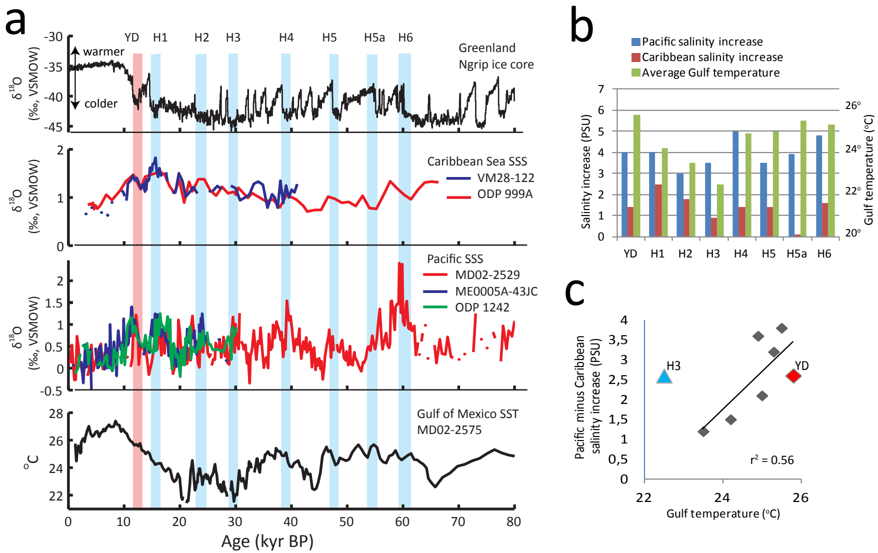

Fig. 7. **(a)** Proxy based evidence for changes in cross-isthmus moisture transport during periods of rapid glacial climate fluctuations. Shown from top to bottom are: Greenland temperatures expressed as δ^{18}O values (NGRIP-Members, 2004), Caribbean SSS (Schmidt et al., 2004), Pacific SSS (Benway et al., 2006; Leduc et al., 2007) and Gulf of Mexico SSTs (Nurnberg et al., 2008; Ziegler et al., 2008). Heinrich events (H1–H6) are indicated by the blue bars, the Younger Dryas (YD) is indicated by the pink bar. **(b)** Surface salinity increases observed on the Pacific and Caribbean side of the Central American isthmus during Heinrich events and the Younger Dryas are expressed as PSU (practical salinity units) following Leduc et al. (2007) (see his Figure SF5 for details). Gulf of Mexico SSTs are calculated as an average during each cold event (Nurnberg et al., 2008; Ziegler et al., 2008). **(c)** Correlation between average SSTs in the Gulf of Mexico and Pacific minus Caribbean salinity increases during Heinrich events (gray diamonds) and the Younger Dryas (red diamond). Heinrich event 3 is indicated with a blue triangle, as only during this event cooling occurred in the Gulf of Mexico (Ziegler et al., 2008). Correlation $r^2 = 0.56$, excluding Heinrich event 3.

CPD
7, 3859–3893, 2011

Two-signed moisture feedback with the glacial AMOC

H. J. de Boer et al.